# Heart Rate Monitoring in Sports

Tiago Miguel Cavaleiro Rodrigues
tiago.m.rodrigues@tecnico.ulisboa.pt
Master of Science Degree in Biomedical Engineering
Instituto Superior Técnico, Lisboa, Portugal

January 2021

**Abstract**

Reliable detection of the R wave in an Electrocardiogram (ECG) signal is a crucial step for further heart rate variability (HRV) analysis, biometric recognition techniques, and additional ECG waveform feature extraction. Here, the ECG signals were acquired using the *FieldWiz* device and a Wearable connected T-shirt in dynamic conditions. The influence of different acquisition setups was estimated, concerning the materials used, hardware, and type of activities.

Several common QRS algorithms were evaluated in a private *FieldWiz* and *Physionet* Databases. A novel real-time and low-complexity R wave detection algorithm was presented. The proposed algorithm was designed, optimized and evaluated in a private annotated database, $N_{subjects} = 5$. The combined acquisition setup and presented approach resulted in R-peak detection Sensitivity (Se) of $99.77\%$ and Positive Predictive Value (PPV) of $99.18\%$ in the *FieldWiz Database*, comparable to the evaluated state of the art QRS detectors. In the *Physionet* Databases, the results revealed to be highly influenced by the QRS waveform, achieving for MIT-BIH (MITDB) a median PPV of $99.79\%$ and median Se of $99.52\%$, with an overall reduced PPV of $98.35\%$ and Se of $97.62\%$. The evaluated method can be implemented in wearable systems for cardiovascular tracking devices in dynamic use cases with good quality ECG signals, achieving comparable results to the state of the art methods. Artefact correction algorithms were evaluated, together with their influence on the HRV metrics.

The detection of R waves from ECG acquired in dynamic contexts showed encouraging results when using a combination of FieldWiz and a Wearable connected T-shirt. Improvements in the signal processing techniques must be conducted, alongside artefact correction from the signal acquisition stage. This work lays the foundations for exploring topics such as sympathovagal modulation from the RR-intervals in dynamic and rigorous environments using wearable devices, in particular, the *FieldWiz*.

**Keywords:** FieldWiz; ECG; HRV; QRS detectors; Wearable Devices

## 1. Introduction

Recently, wearable devices and big data have revolutionized the concepts of health care, sports and lifestyle. The ubiquity of connected devices, together with improvements in data transfer and management, have transformed the interactions between users and healthcare providers, likewise, the training plans and feedback between coaches and athletes. Amongst the different physiological signals, the electrocardiogram (ECG) is the most extensively studied.

In sports, the most commonly used metric is the heart rate (HR). While other features, such as heart rate variability (HRV), are often overlooked. These HRV metrics derive from the study of the time differences between consecutive heartbeats, also known as RR-intervals. They have been receiving increased attention and correlations have been made between HRV and emotion [14], stress-management [26], or as a discriminator for patients with psychological disorders [10].

Widely established correlations between training load and HR(V) have been used for train planning [21] and, more recently, HR(V) based training has even shown increased performance in road cyclists [11]. Recent studies have also focused on correlations between HR(V) metrics and emotional intelligence, used as a metric to understand how athletes cope with in-game stress [13]. A recent in-depth review [3] has stated that contradictory findings in HRV studies are likely to be related to methodological inconsistencies or misinterpretations of the data, rather than a limitation of heart rate measures as a proxy to inform on the subject physiological status.

The use of HR(V) metrics is relevant in two distinct groups, individual and collective sports. In individual sports, an HRV index should be measured at least 3 to 4 times a week. Besides, HR should be measured weekly, one time during exercise and one time during recovery. On the other hand, HR(V) based training is still limited to team sports. Limitations from HR(V) include: 1) HR measures cannot inform on all aspects of wellness, fatigue and performance; 2) Lack of understanding

between HR and neuromuscular/metabolic/physiological mechanisms and 3) HR measurements are usually taken using chest straps, which are more uncomfortable to players than regular vests. Currently, the gold standard for HR(V) monitoring in the context of sports is still the traditional chest straps with the widely used Pan and Tompkins [11]. These are more uncomfortable when compared to wearable vests and cannot be used in certain scenarios (e.g. FIFA regulated games). Other wearable devices such as connected T-shirts have also been proposed, however, these are still not considered reliable for HR monitoring.

Ultimately, the research goal of this work was to assess the feasibility of implementing a real-time R-peak detector, robust in noisy environments, capable of coping with fast changes in HR. As well as, evaluate the reliability of the measurements. Which, in turn, can be used to further study the relations between HRV, psychophysiological states, emotional stress and fatigue.

## 2. Background

The practical real-time detection of the QRS complex was introduced by Pan and Tompkins [12]. Since then, several algorithms for QRS complex detection have been proposed. Generally, these consist of a pre-processing step for QRS enhancement, followed by a decision stage. Enhancement may be achieved through amplitude-based methods, derivative, digital filters, empirical mode decomposition (EMD) or Wavelet Transform. Subsequently, detection can make use of threshold-based methods, neural networks or matched filters [5]. Some of these methods are either computationally expensive, hence not suitable for real-time applications, or computationally demanding to use in embedded systems. Thus, some of the most common real-time QRS complex detectors also used in this study were Pan and Tompkins [19], Christov [4], Gamboa [8] Elgendi [6], Engelse and Zeelenberg [18] and Kalidas [12]. In the context of wearable devices, these include baseline wander, sudden drift and loss of contact due to movement of the electrodes [1]. A recent review [5] pointed out that derivative filters for QRS complex enhancement, combined with adaptive threshold, are still the most simple, computationally efficient yet reliable approach. These are consistent with findings in [16], where derivative-based detectors had similar high F1 scores amongst ECG with reasonable to good signal quality. Nevertheless, if one wants to study HRV, the R-peak detectors should be carefully selected, as recommended in [20]. In this study, from different approaches examined, only the approach by Engelse and Zeelenberg modified and Stationary Wavelet Transform (SWT) based for noise removal by Kalidas achieved accurate R-peak detection. These either exploited local search for the R-peak or used wavelet decomposition for noise removal, preserving the QRS complex waveform.

Limitations of the Engelse and Zeelenberg are the lack of robustness to noise, varying heart rate and R-peak amplitude changes. Also, this method is not suitable for ECG signals with inverted polarity. Contrarily, the noise removal based on stationary wavelet transforms implemented in real-time yields promising results for quasi-real time applications with the noise removal and thresholds being applied in 3 second ECG buffers. This method requires a learning stage, the initial 10 seconds, where the signal is assumed to be clean or the performance will be affected. In commercially available software, the R-peak is usually extracted using adaptations of the Pan-Tompkins with local search for maximum, once the QRS complex is detected. Nevertheless, a modification of Pan-Tompkins with local R-peak search has a complex implementation and may not be suitable in cases where resources and memory allocation are limited.

## 3. Methodology

### 3.1. Acquisition System

The quality of the acquired ECG signals was evaluated through a preliminary study using different acquisition setups. Different configurations used were a combination of 1) *Wiz* connected T-shirt, Version 1 with *FieldWiz*; 2) *Wiz* connected T-shirt with Version 2 and *FieldWiz* and 3) *Admos* Live with gel electrodes. Both devices, connected T-shirts and electrode placement are illustrated in Figure 1.

The electrode pads from the T-shirt Version 1, shown in Figure 1a) were placed in the chest, under the pectoral muscles. While the electrode pads, when using the T-shirt Version 2, shown in Figure 1b) rested in a lateral position. Improvements from the later version of the T-shirt in comparison to Version 1 are the different conductive fabric, the positioning of the electrode pads, and the elastic fit. The improved lead placement shown in Figure 1e) is known to be significant to reduce motion noise and movement artifacts, in particular, under extreme conditions, where artifacts from muscle contractions and motion are a source of noise contamination [7].

#### 3.1.1 Signal Quality Index (SQIs)

In this work, the signal quality was evaluated using a Signal Quality Index (SQI) approach based on simple heuristic fusion described in [25]. The selection of this method relied on the good performance in selected Physionet Databases (Physionet/Cinc Challenge 2017 and Physionet/Cinc Challenge 2011) and comparable Accuracy (Acc) and Specificity (Sp) to previous methods [25]. The index made use of common signal quality metrics described in the literature. It adopted four synthesized signal quality indexes, these were *qSQI*, *pSQI*, *kSQI* and *basSQI*, described as the following.

**qSQI**, signal quality index based on the ability to detect the QRS complexes using two different methods. $qSQI = \frac{2N}{N_1+N_2}$, where $2N$ is the number of R-peaks detected in the number of R-peaks in the interval and $N_1$

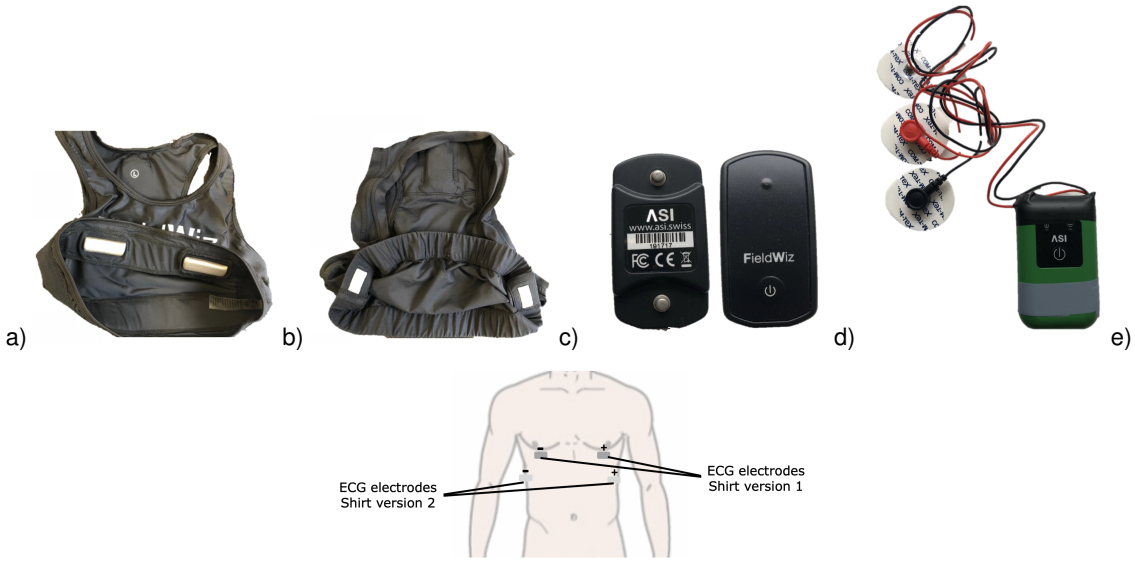


**Figure 1:** Acquisition Setup. (a) Wiz connected T-shirt, Version 1; (b) Wiz connected T-shirt, Version 2; (c) FieldWiz device; (d) Admos Live and (e) ECG electrode pads placement for the different Versions 1 and 2 of the connected T-shirt.

and $N_2$ are the number of QRS complexes detected using the first or the second method, respectively.

**pSQI**, based on the evaluation of the power spectrum distribution of QRS wave. The index is given by $pSQI = \frac{\int_{f=5Hz}^{f=15Hz} P(f)df}{\int_{f=5Hz}^{f=40Hz} P(f)df}$, the quotient of the signal energy of the QRS band [5,15] Hz, with the rest of the signal [5,40] Hz.

**kSQI**, based on the kurtosis of the signal, which measures the relative peakedness of a distribution with respect to a Gaussian distribution. From the central limit theorem, independent random processes tend to have a normal distribution. For clean signals, the asymmetrical distribution results in increased kurtosis values. Contrarily, in the presence of baseline wander or powerline interference, the kurtosis is decreased.

**basSQI**, from the relative power of the baseline drift $basSQI = \frac{1-\int_{f=0\text{Hz}}^{f=1\text{Hz}} P(f)df}{\int_{f=0\text{Hz}}^{f=40\text{Hz}} P(f)df}$. A low *basSQI* means that the power within [0,1Hz] is high with respect to the power in the [0,40Hz] band.

Based on a simple fusion of the four heuristic metrics, each segment was evaluated and classified as either '*Optimal*, *Suspicious* or *Unqualified*'. Later, from the classification of each computed $SQI$, the 10 seconds ECG segments were characterized as either *Excellent (E)*, *Barely Acceptable (B)* and *Unacceptable (U)*, as a result from $SQI$ ($qSQI, pSQI, kSQI$ and $basSQI$) described in [25].

## 4. Results & discussion

### 4.1. Comparison: Wiz T-Shirt Version 1 and Version 2

The comparison between the two different T-Shirt versions was done using two selected recordings and making use of SQIs. T-shirt Version 1, *Recording: 20200205-TR-FWv1.txt* and T-shirt Version 2, *Recording: 20200301-TR-FWv2.txt*. The raw ECG signal was divided into 10-second epochs as input for the SQI evaluation.

The signal acquired using Version 1 of the T-Shirt showed poorer results when benchmarked against Version 2 using the described SQI. The initial transients and noisy regions of the signal were classified as Unacceptable ($U$), additionally, the overall signal quality oscillated between Barely Acceptable ($B$) and Unacceptable ($U$), resulted in $B = 48.1\%$ and $U = 51.9\%$.

In turn, the signal acquired using Version 2 of the T-shirt showed increased signal quality when evaluated with the same combination SQIs. In this test, the metrics registered values of $B = 65.9\%$ and $U = 34.1\%$.

The ratio $B/U$ was increased from Version 1 = 0.93 to Version 2 = 1.93, thus, from the combination of the studied indexes ($qSQI, pSQI, kSQI$ and $basSQI$), the results suggested that Version 2 has comparatively better ECG signal quality when compared to Version 1.

### 4.2. Comparison: Water, No Water and Electrode Gel

The combination of FieldWiz and Wiz connected T-shirt Version 2 were evaluated using different electrode-skin interfaces. The results from not moisturizing the electrode pads, applying water or using electrode gel are shown in Figure 2 for the recordings: *20200420-JT-FWv2.txt, 20200421-JT-FWv2.txt* and *20200422-JT-FWv2.txt*, respectively. The use of water and electrode gel showed comparatively better results to the no use of water. Additionally, using electrode gel showed consistent saturation, likely due to the lack of skin/electrode adhesion.

### 4.3. State of the Art QRS detectors

Some of the commonly used QRS complex detectors evaluated in this study were the original Pan and Tompkins [19], Christov [4], Gamboa [8], Engelse and Zeelenberg modified [18], Elgendi [6] and Kalidas [12].

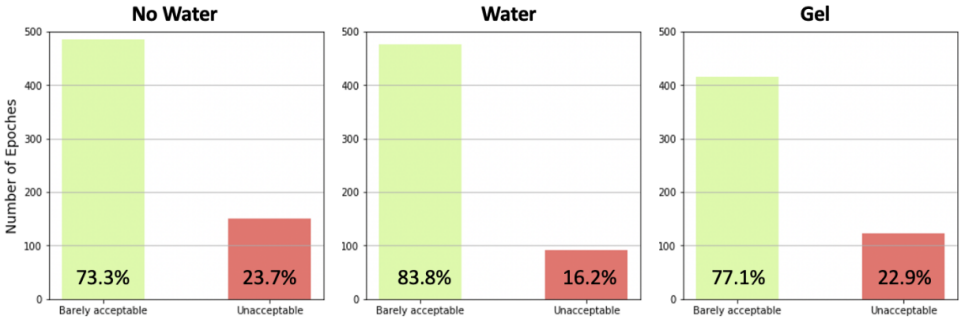


**Figure 2:** ECG quality assessment. Signal acquired using the *FieldWiz* and the Wiz connected T-shirt Version 2, under different settings. a) Without application of water to the electrode pads, Recording: 20200420-JT-FWv2.txt; b) Moisturizing the pads with water, Recording 20200421-JT-FWv2.txt and c) Applying electrode gel, Recording: 20200422-JT-FWv2.txt.

From initial observation, Gamboa and Elgendi revealed to be less robust to different signal conditions and resulted in an increased number of missed/false beat detections. Visually, the detectors that showed the best sensitivity under physical activity were the Pan and Tompkins, Christov, Engelse, and Zeelenberg (Engzee), and Kalidas. From these, the Pan and Tompkins introduced changes in the temporal precision of the R-peak, despite its robustness as a QRS detector. On the other hand, the annotations by Kalidas showed a consistent delay from the R-peak of 2/3 samples. The approach by Engzee modified [18] also showed good temporal precision of the R-peak detection.

#### 4.3.1 Proposed Approach

From the preliminary results, the principal sources of noise under dynamic conditions when using a combination of the FieldWiz and the connected T-shirt were baseline wander, enhanced T-waves, occasional loss of contact between the skin/electrodes and saturation. Subsequently, two consecutive derivative steps were used to remove low-frequency noise and T-wave, while enhancing the QRS complex. Recent approaches for QRS complex and R-peak detection using these schemes have shown promising results [9] and [22].

The proposed approach builds upon these two methods, combining an adaptation of the temporal precision of the double derivative pre-processing method for R-peak detection, with the simple and numerically efficient Finite State Machine (FSM) approach. The full block diagram of the pre-processing and detection pipeline of the algorithm are shown in Figure 3a).

It is divided in a pre-processing stage and a detection stage:

**Pre-Processing Stage (3 steps)**:

1) A derivative step, of *N* samples, was implemented to reduce low-frequency noise (e.g. baseline wander), suppress pronounced T-waves and enhance the QRS complex. The resulting signal, $y_1[n]$, was characterized by high values associated with the QRS complex and an inflexion point at the R-peak. A second derivative was used to isolate the R-peak position, which resulted either a local maximum or minimum, depending on the signals' polarity.

2) Squaring, non-linear enhancement, isolated the R-peak and eliminated the effect of variable polarities.

3) Integration window, moving integration of $N$ samples. Reduced source of noise and optimized for detection of events with similar duration as the QRS complex.

The pre-processing stage is described by Equations (1) to (4).

The derivative and integration window steps, Equation (1) and (4), considered $N = 5$, value optimized for a sampling frequency of 250 Hz, which corresponded to a 20 ms interval, i.e. a time-window comparable to half of the R-peak slope [9]. Additionally, the order of these two operations revealed to influence the temporal precision of the R-peaks.

$$y_1[n] = x[n] - x[n-N] \tag{1}$$

$$y_2[n] = y_1[n] - y_1[n-1] \tag{2}$$

$$y_3[n] = (y_2[n])^2 \tag{3}$$

$$y[n] = \frac{1}{N}\sum_{k=0}^{N} y_3[n-k] \tag{4}$$

**Detection Stage (3 states)**, illustrated in Figure 3b) (adapted from [9]):

State 1) Search for the absolute maximum in a time window of $RR_{min}$ = 200 ms in the processed ECG signal, $y[n]$. The maximum value, which corresponded to the R-peak position, $R_{peak}Pos$, was saved.

State 2) Idle state, replicating the refractory period of the heart. Prevented false detection of additional R-peaks in the following $RR_{min}$ = 200 ms after one detection. Afterwards, the adaptive threshold was computed from the average of the last 20 R-peaks amplitudes, adaptively coping with changes in R-peaks amplitude, e.g. resulting from different exercise conditions [23].

State 3) Detection threshold value decayed exponentially, following Equation 5, where $T_s$ is the inverse of the sampling frequency and $P_{T_h}$ is a free parameter.

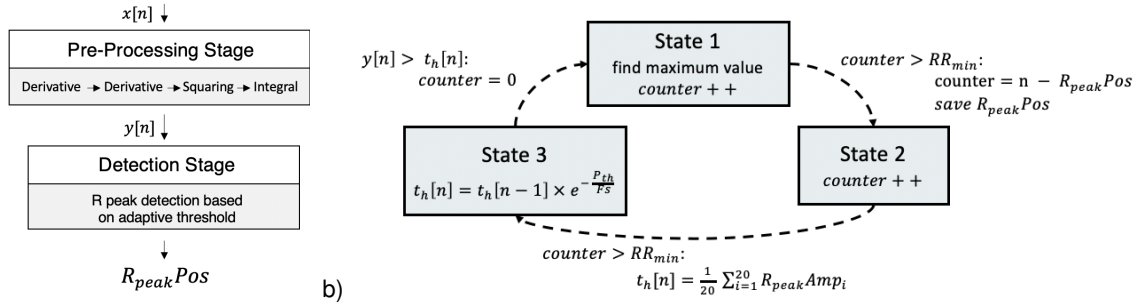


**Figure 3:** Schematics of the proposed R-peak detector. a) Block Diagram of the algorithm and b) Representation of the Finite State Machine. Adapted from [9].

The state ended when the processed signal, $y[n]$, exceeded the threshold signal, $t_h[n]$. Then, the state and the counter are renewed, and a new search for the R-peak is triggered.

$$t_h[n] = t_h[n-1] \times e^{-P_{T_h} * T_s} \tag{5}$$

The R-peak amplitude showed to vary throughout a recorded session, especially during dynamic activities. This occurred not only as a result of changes in conductivity from perspiration, ambient, or skin temperature but also motivated by physiologic changes from varying exercise intensities. In [2], the first correlations were made between R-amplitude at rest and peak exercise, showing a significant decrease of the mean amplitude of the R-peak of normal individuals, at peak exercise. Thus, the proposed changes include an adaptive detection threshold $t_h$, resulting from the average of the last 20 R-peak amplitudes, instead of the average of all previous detected R-peaks amplitudes.

Furthermore, the free $P_{th}$ parameter, previously optimized using ECG databases in resting conditions, was adapted for our use case. These modifications are illustrated in Figure 3.

#### 4.4. FieldWiz Private Database

The QRS detection algorithms were evaluated in a private FieldWiz ECG database. The raw ECG signals were collected using a combination of *FieldWiz* and both connected *Wiz* T-shirt Version 2 and chest strap.

The five recordings were collected from four different subjects under different conditions, using the FieldWiz device combined with the Wiz T-shirt Version 2 (FWv2) and a chest strap (Belt). Recordings: *20200405-TR-FWv2.txt*, 30 min running; *20200413-JM-FWv2.txt*, 60 min running; *20200421-JT-FWv2.txt*, 60 min trail running; *20200505-TR-Belt.txt*, 30 min high intensity interval training (HIIT); *20200508-SS-Belt.txt*, 40 min run.

The acquisitions took place in different days, according to the following: 1) The electrode pads in the T-shirt and chest strap were moisturized before the activity to increase the conductivity of the fabric; 2) The T-shirt and chest strap were well secured, the electrode pads were located under the pectoral muscles (when using chest strap) and lateral part of the torso, when using the Wiz T-shirt. The different activities accounted for heart rate values ranging between 60 bpm, during the resting stage, and up to 190 bpm during the maximal HR.

The raw ECG signals were recorded, saved and later exported as .txt files. Next, the ECG signals were automatically annotated using the detection method by Kalidas [12] for automatic R-peak detection, and the raw ECG signals were stored together with the R-peak annotations as an HDF5 file. The HDF5 file format was selected to interface with the web-based annotation tool SignalBit [17]. Later, the annotations were visually inspected by a cardiopneumologist technician and manually corrected by either removing false-positive R-peaks or adding false-negative R-peaks. It was noted that the implemented detection approach by Kalidas resulted in detected R-peaks with small sample imprecision (varying up to 2 samples around the inflexion point, corresponding to an 8 ms time-shift at 250 Hz sampling frequency). These imprecisions were accounted for, by choosing an acceptance window of 5 samples, corresponding to 20 ms, in Section 4.4.2.

##### 4.4.1 Parameter Optimization

The method introduced is comprised of a derivative step of $N$ samples and a detection threshold with exponential decay proportional to $P_{th}$.

A sensitivity analysis was performed to choose these parameters. The means ($\mu$) and means' standard deviations ($\delta$) of Sensitivity (Se) and Positive Predictive Value (PPV), across the different recordings, were computed. The mean values from the parameter optimization for different values of $P_{th}$ and $N$ are shown in Figure 4.

The Se and PPV were calculated as per Equations (6) and (7), considering the true positive detected beats (TP), the false negative detected beats (FN) and the false positive detected beats (FP).

$$Se = \frac{TP}{TP+FN} \tag{6}$$

$$PPV = \frac{TP}{TP+FP} \tag{7}$$

One limitation of the approach by Gutierrez [9] is building upon the optimization of $P_{th}$ using ECG databases

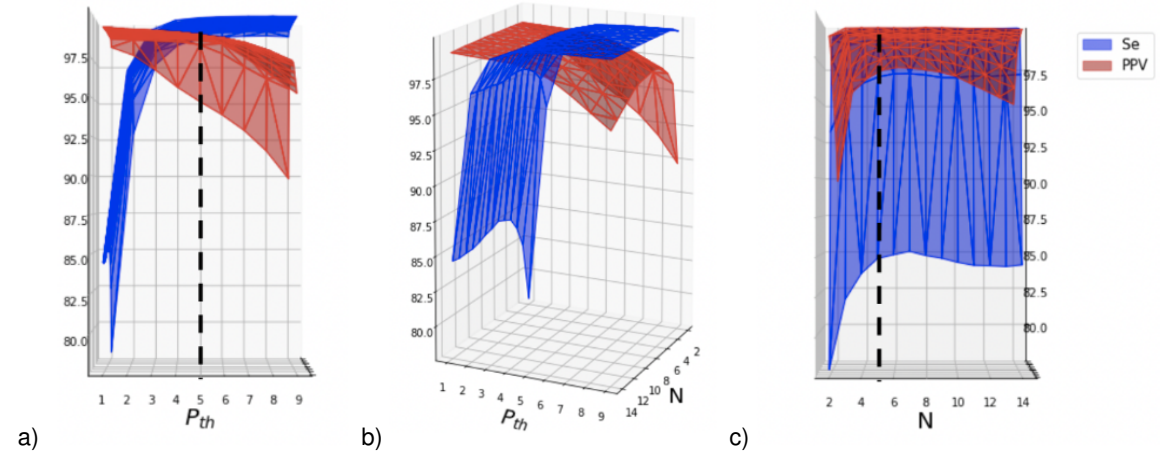


**Figure 4:** Parameter optimization ($P_{th}$ and $N$), Sensitivity (Se, blue) and Positive Predictivity (PPV, red) planes. a) Se and PPV with varying $P_{th}$; b) Transverse plane and c) Se and PPV with varying $N$. The selected values of $P_{th}$ = 5 and $N = 5$ are represented by the black dashed line.

with resting HR. Thus, while lower $P_{th}$ is suitable for lower heart rate, higher Se is needed for higher HR values.

From Figure 4a), it is noticeable Se and PPV are influenced by the decay of the threshold, proportional to $P_{th}$. Lower values of $P_{th}$, associated with a slower decaying detection threshold, resulted in decreased Se values (as low as 80% for $P_{th}$ = 1) while achieving the highest PPV values. The Se increased with $P_{th}$, until it intersected with PPV at around $P_{th}$ = 4 and the PPV value decreased. Overall, the $P_{th}$ curves showed a similar performance for each value of $N$ in the range of $4 < N < 12$.

In Figure 4c), the influence of the first derivative step is shown. Lower values of $N$ (e.g. $N = 2$, corresponding to an interval of 8 ms), are not convenient to enhance the QRS complex, thus showing the highest number of False Positives for different values of $P_{th}$. Also, Se increases with $N$, until a maximum of around $N = 7$. The parabolic dependency on Se on $N$ is not uniform, and so, an $N = 5$ was chosen (20 ms, approximately a quarter of the QRS complex duration), compromising sensitivity for increased temporal precision of the R-peak location.

Lastly, Figure 4c) demonstrates the relation between Se and PPV for a region of parameters. The subset of parameters in the range of $3 < P_{th} < 5$ and $4 < N < 8$, achieved Se and PPV values higher than 98%. Finally, the $P_{th} = 5$ and $N = 5$ were chosen from the trade-off between Se, PPV, and temporal precision of the detected R-peaks.

#### 4.4.2 FieldWiz Database

The detected peaks were compared against the benchmarked annotations. Acceptance windows of 25 and 5 samples were used, corresponding to 100 ms and 20 ms acceptance windows, respectively. The window of 100 ms was selected to evaluate the different detectors ability to find QRS complexes in the ECG signals recorded. After, a window of 20 ms was chosen to evaluate the temporal precision of the detection. While accounting for imprecisions in the annotation method. The results are shown in Figure 5 for the respective 100 ms in Figure 5 a) and 20 ms in Figure 5 b). The resulting means ($\mu$) and standard deviations ($\delta$) are summarized in Table 1. The signals with inverted R-wave, as a result of the lead placement, were reverted to account for the limitations of the method by Engzee [18].

From Figure 5a), when using a wider detection window of 100 ms, the methods by PanTompkins, Kalidas and the proposed method achieved Se values $>$ 99% (green), Engzee equal to 96.16% (yellow) while Elgendi and Gamboa showed the worst performance with 72.88% and 63.98% (red), respectively. The PPV was $>$ 99% in PanTompkins, Engzee, Kalidas and proposed (green), Christov with 93.95% (yellow) and underperforming are Elgendi and Gamboa at 81.82% and 56.23% (red).

Overall, the results showed that the signal quality using the combination of the FieldWiz and Wiz shirt or chest strap, under the dynamic conditions studied is suitable for QRS detection using any of the previous methods PanTompkins, Kalidas, or the proposed approach with Se and PPV values $>$ 99%. Also, from Figure 5b), decreasing the time detection of the acceptance window for 20 ms yielded good results for Kalidas and the proposed approach $>$ 99% Se and PPV (green), satisfactory results for Enzee (yellow), while notably decreased performance for PanTompkins, Christov and Gamboa (red) for both Se and PPV. The performance of the Engzee method did not suffer significative differences.

Ultimately, the method by Kalidas, the proposed approach, or a combination of PanTompkins with an additional local search for the inflexion point for the R-peak, would yield good results.

#### 4.5. Physionet Databases

The proposed detector was evaluated against common Physionet databases. The annotations were retrieved using the *Physionet WFDB* wrapper for $MATLAB$. Since

**Table 1:** R-peak detections Sensitivity (Se) and Positive Predictive Value (PPV) and respective means ($\mu$) and standard deviations ($\delta$) for the different QRS detectors (Pan and Tompkins, Christov, Gamboa, Elgendi, Engzee, Kalidas and the proposed approach). TABLE 1a using a detection window of 100 ms to the annotated R-peaks and TABLE 1b a detection window of 20 ms.

**(a)** Detection window of 25 samples (100 *ms*).

| Method | Se ($\mu$) | Se ($\delta$) | PPV ($\mu$) | PPV ($\delta$) |
|---|---|---|---|---|
| PanTompkins | 99.34 | 0.43 | 99.04 | 1.50 |
| Chistov | 99.07 | 0.61 | 93.95 | 5.20 |
| Gamboa | 63.98 | 9.21 | 56.23 | 12.02 |
| Elgendi | 72.88 | 19.16 | 81.82 | 13.21 |
| Engzee | 96.16 | 5.72 | 99.25 | 1.29 |
| Kalidas | 99.90 | 0.11 | 99.27 | 1.37 |
| Rodrigues | 99.77 | 0.23 | 99.18 | 1.52 |

**(b)** Detection window of 5 samples (20 *ms*).

| Method | Se ($\mu$) | Se ($\delta$) | PPV ($\mu$) | PPV ($\delta$) |
|---|---|---|---|---|
| PanTompkins | 32.23 | 9.43 | 32.04 | 9.19 |
| Chistov | 84.96 | 10.93 | 80.53 | 11.44 |
| Gamboa | 56.53 | 10.87 | 49.83 | 13.12 |
| Elgendi | 70.29 | 20.50 | 78.71 | 15.10 |
| Engzee | 95.71 | 5.543 | 98.80 | 1.75 |
| Kalidas | 99.85 | 0.12 | 99.23 | 1.37 |
| Rodrigues | 99.64 | 0.28 | 99.06 | 1.60 |

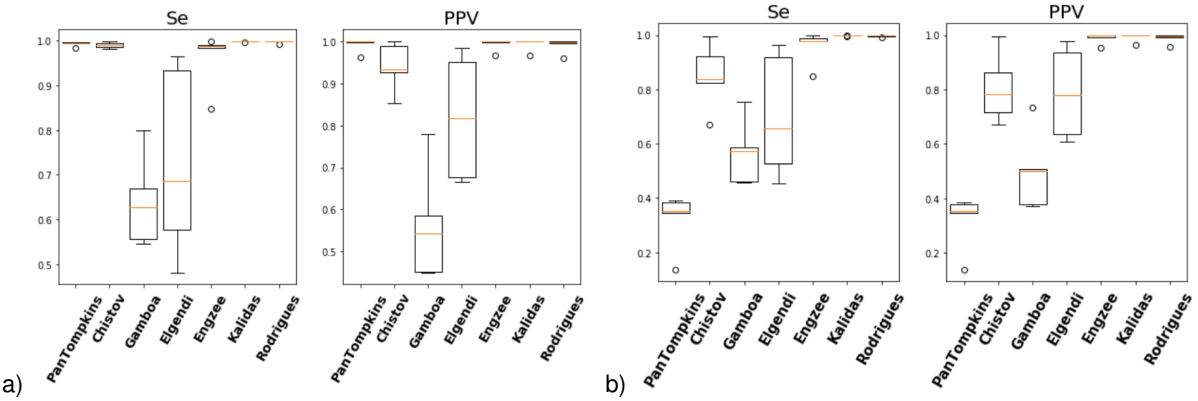


**Figure 5:** Evaluation of the different QRS detectors: PanTompkins, Christov, Gamboa, Elgendi, Engzee, Kalidas and proposed approach (Rodrigues). Sensitivity (Se) and Positive Predictivity Value (PPV) using FieldWiz private dataset. Using a detection window of a) 100 ms and b) 20 ms.

the detection ground truth does not implicitly return the same sample as the correspondent annotation, a detection margin of 100 ms was added to the acceptance window and all non-beat annotations were excluded.

The parameter $N = 5$ for the derivative and moving integration was selected based on the sampling frequency, corresponding to a 20 ms differentiating step, as detailed in [9] and a sensitivity analysis was done for $P_{th}$. The results are showed for $P_{th} = 3$, resulting from the compromise between Se and PPV. The results are shown in Table 2. It was noticeable that the QRS complexes from different individuals had various degrees of variability, especially between patients and healthy subjects. In the case of arrhythmias, the resultant different QRS waveforms increased detection difficulty. Besides, irregular heart rate was an additional source of error.

A recent review on ten of the most computationally efficient QRS detectors [16] showed that the accuracy of derivative-based QRS detection methods did not decline significantly for arrhythmia databases when considering the mean of the entire dataset. However, our results suggest that each record should be analyzed individually for clinical applications since the Se and PPV might decline drastically with distinct waveforms. The PPV and

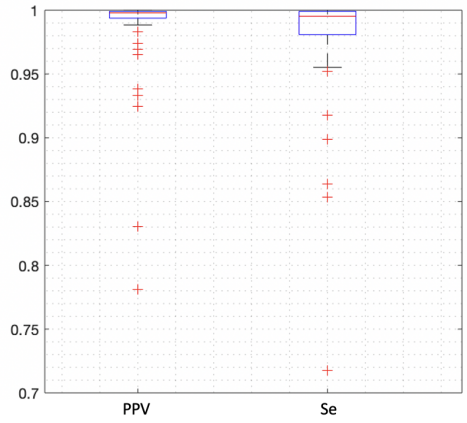


**Figure 6:** Evaluation of the R-peak detector using MIT-BIH Arrhythmia Database (mitdb). PPV and Se boxplot of the 48 records with respective median (red line), 25th and 75th percentile (black lines) and outliers ( red '+' symbol).

Se boxplots for the MIT-BIH (mitdb) are shown in Figure 6. Resulting in PPV (median = 99.79%, outliers $<$ 95% id: 108, 203, 207, 228, 232) and Se (median = 99.52%, outliers $<$ 95% id: 106, 203, 208, 221, 223).

**Table 2:** Summary of the results obtained (TP, FP, FN, PPV (%) and Se (%)) using the proposed algorithm in the considered databases. For benchmarking we used Pth = 3 & N = 5 as parameters of the algorithm.

| Database | Sampling Rate (Hz) | TP | FP | FN | PPV (%) | Se (%) |
|---|---|---|---|---|---|---|
| Challenge 2014 | 120-1000 | 71529 | 332 | 884 | 98.88 | 99.52 |
| ST-T Database (ltstdb) | 250 | 782483 | 13712 | 8082 | 98.15 | 98.79 |
| MIT-BIH (mitdb) | 360 | 106590 | 1758 | 2904 | 98.35 | 97.62 |
| MIT-BIH (nstdb) | 360 | 23957 | 2907 | 1633 | 96.23 | 98.72 |

#### 4.6. Heart Rate Variability

Even though heart rate (HR) and heart rate variability (HRV) metrics are believed to reflect some physiological and psychological responses, they cannot inform on all aspects of fatigue and performance as they are influenced by several internal and external confounding factors [3].

The presence of artefacts such as ectopic missed, or extra beats, is highly impactful when estimating the heart rate variability metrics. Recently, the increased quality of the recorded ECG signals due to hardware improvements, combined with better R-peak detection has mitigated the presence of errors and artefacts when evaluating HRV. Nonetheless, correcting RR-intervals series is still of great importance in ambulatory environments, extreme conditions and when using wearable technology. In common practice, for an accurate HRV analysis, the raw ECG are recorded and the annotated events are edited using private or publicly available software for artefact detection and correction.

In this study, three different correction approaches were considered: 1) No artefact correction; 2) Beat removal if the RR-intervals deviated more than 20% from the RR-intervals 15 points moving median. These were then corrected by interpolating the RR time series using cubic spline interpolation and 3) A novel artefact correction algorithm for HRV, based on a set of decision rules for beat classification [15], implemented in Kubios software [24]. The decision rule pipeline, classified the beats as either normal, ectopic, missed/extra, or long/short and corrected accordingly. The effects of ectopic beats were diminished by replacing erroneous RR-intervals by interpolated values. Missed and extra beats were amended by either adding or removing RR-intervals. Long or short beats were revised by adding new interpolated values in the RR series.

The R-peak proposed detection method was used to extract the R-peaks from the ECG signal. The resulting RR-intervals, as well as other common time and frequency domain metrics, were computed. The RMSSD and normalized HF and LF were computed over 10 and 120 seconds epochs, respectively. Different values for both time and frequency domain metrics were observed when using distinct correction methods. When used in high Heart Rate situations, results suggested that the correction method from Kubios correction resulted in misclassified events. Ectopic beats, classified as missed beats, were consequently classified as missed beats and interpolated instead of additional beats being added. Hence, resulting in artefacts in the time-domain and less visible in the normalized HF and LF.

Overall, choosing either one of the approaches is preferred to the no use of any artefact removal, as the differences introduced in both time and frequency domain were negligible. Nevertheless, these methods should be carefully used, for instance, for beat classification e.g. classification of ectopic beats during exercise.

#### 4.7. Implementation

Following the offline validation, the R-peak detection algorithm from Section 4.3.1 was implemented in C and embedded in the FieldWiz device. The device is a 32-bit microcontroller based on ARM architecture with a Cortex-M4 processor.

The R-peak detection was implemented in real-time and the detected peaks were stored in the flash memory. In order to extract the HRV metrics, the pre-processing pipeline implemented in the *MATLAB* server followed the results discussed in Section 4.6.

The implemented artefact removal method had to remove any unwanted missed/extra or ectopic beats while maintaining the original RR-intervals, which excluded the common operations such as moving median/average, interpolation, or digital filtering. The RR-intervals were removed from the time series based on the decision criterion from the distance to the running median. If this distance was larger than 30% threshold from running median of the last 15 RR-intervals, $\widetilde{RR}_{15}$, the RR-interval is replaced by $\widetilde{RR}_{15}$.

Following the R-peak detection and artefact correction, the RR-intervals and HRV Time and Frequency domain metrics were calculated in the *MATLAB* using custom scripts, using 120 seconds of RR-intervals intervals, as recommended in [3].

## 5. Conclusions

The *FieldWiz* device and different versions of the Wiz connect T-shirt were evaluated in different settings, from rest to dynamic conditions.

**Signal Quality Evaluation**

Using well-established *SQIs*, comparisons between

the Signal Quality of the Version 1 and Version 2 of the T-shirt were performed. The signal-to-noise ratio (SNR), measured as $B/U$, increased significantly from Version 1 to 2 (Version 1 = 0.93 and Version 2 = 1.93). Version 2 showed comparatively better ECG signal quality, probably resultant of the improved material, lead placement and elastic fit.

A comparison between different acquisition setups was evaluated using the previously mentioned SQI. Applying water to the electrode pads, without water and using electrode gel. The use of electrode gel often resulted in saturation, one possible reason was attributed to the loss of adherence between the skin and electrode pads. Overall, in regions without saturation, the SNR did not differ when using water in comparison to the use of electrode gel. Finally, the use of water or electrode gel is preferred over the use of no water.

The results from the dynamic tests suggested that challenging scenarios associated with motion artefacts e.g. rugby can compromise the reliability of the results when using wearable T-shirts. In these cases, the use of a chest strap or a PPG watch is preferred.

**QRS detectors**

Six commonly used QRS detectors were evaluated and a novel proposed approach was introduced. The latter, consisted of a pre-processing stage based on the double derivative and a detection stage based on an FSM. The method has a low computational load and memory allocation and it is fairly simple to implement, allowing its implementation in an embedded system.

Advantages of the proposed approach include:

1) Robust to different R-wave polarities, contrary to the approach by Engelse and Zeelenberg modified;

2) Pre-processing based on the double derivative increase R-peak precision when compared to the original FSM approach [9];

3) Increased sensitivity, due to the adaptive exponentially decaying threshold for highly dynamic and fast-changing heart rate and R-peak amplitudes settings, when compared with PanTompkins, Christov, Engzee and Gamboa; and 4) Real-time deployment, when compared to the quasi-real-time approach by Kalidas [12] using stationary wavelet transform in ECG buffers of 3 seconds. The main limitations and additional points to be investigated are:

1) Parameter $P_{th}$ was optimized in a dataset ($N_{subjects} = 5$) with heart rate varying from 60 bpm to 190 bpm, building upon the future use cases of the device; lower heart rates (e.g. 40 bpm), may lead to increased False Positives (FP) and higher rates (e.g. 200 bpm), may result in False Negatives (FN). Further evaluation using a larger database should be done. The values of Se and PPV resulted in values $>$ 98% for a range of 4 $<$ N $<$ 8 and 3 $<$ Pth $<$ 5;

2) Individual ECG waveforms are assumed to be time-invariant; the R-peak is shown to be located in the same position of the ECG waveform for every heartbeat. Nonetheless, in pathological conditions with time-varying QRS morphologies, the introduced artefacts will affect heart rate variability related metrics (HRV);

There is a lack of more extensive validation of the different QRS detection methods under highly dynamical activities, resulting from the shortage of ECG databases in these conditions. This work aims at exploring the use case limitations of the current approaches, as well as providing an alternative validated approach that can be used for R-peak detection.

**Heart Rate Variability**

Given that most of the vagally-mediated heart rate variability (HRV) power is focused in [0,1] Hz band, usually, any of the evaluated detectors can be used to determine the distance between the RR-intervals, i.e. successive QRS complexes.

Different artefact correction approaches were evaluated. The correction of beats by removing outliers with respect to the simple statistics (running median) was implemented. The algorithm classification by Kubios was studied as a novel method to classify beats in misclassified false positive ectopic beats under high heart rate conditions. Further tests should be done in larger range of subjects to validate the classification effectiveness in dynamic conditions.

**6. Acknowledgments**

The author would like to thank Prof. Hugo Silva for the discussions and counselling, Prof. Ana Fred for the guidance and Prof. Lionel Yersin for the opportunity to work on this topic.

This work has been partially funded by FCT/MCTES through national funds and when applicable co-funded EU funds under the project UIDB/50008/2020 NICE-HOME.

**References**

[1] U. R. Acharya, S. M. Krishnan, J. A. Spaan, and J. S. Suri. *Advances in Cardiac Signal Processing*. Springer, 2007.

[2] A. Battler, V. Froelicher, R. Slutsky, and W. Ashburn. Relationship of QRS amplitude changes during exercise to left ventricular function and volumes and the diagnosis of coronary artery disease. *Circulation*, 60(5):1004–1013, 1979.

[3] M. Buchheit. Monitoring training status with HR measures: Do all roads lead to Rome? *Frontiers in Physiology*, 5(FEB):1–20, 2014.

[4] I. I. Christov. Real time electrocardiogram QRS detection using combined adaptive threshold. *BioMedical Engineering Online*, 3:1–9, 2004.

[5] M. Elgendi, B. Eskofier, S. Dokos, and D. Abbott. Revisiting QRS detection methodologies for portable, wearable, battery-operated, and wireless ECG systems. *PloS one*, 9(1), 2014.

[6] M. Elgendi, B. Eskofier, S. Dokos, and D. Abbott. Revisiting QRS detection methodologies for portable, wearable, battery-operated, and wireless ECG systems. *PLoS ONE*, 9(1), 2014.

[7] J. Francis. ECG monitoring leads and special leads. *Indian Pacing and Electrophysiology Journal*, 16(3):92–95, 2016.

[8] H. Gamboa. *Multi-Modal Behavioural Biometrics Based on HCI and Electrophysiology*. PhD dissertation, Universidade Técnica de Lisboa, Instituto Superior Técnico, 2008.

[9] R. Gutiérrez-Rivas, J. J. García, W. P. Marnane, and A. Hernández. Novel real-time low-complexity QRS complex detector based on adaptive thresholding. *IEEE Sensors Journal*, 15(10):6036–6043, 2015.

[10] S. J. Hong, D. Lee, J. Park, K. Namkoong, J. Lee, D. P. Jang, J. E. Lee, Y.-C. Jung, and I. Y. Kim. Altered heart rate variability during gameplay in internet gaming disorder: the impact of situations during the game. *Frontiers in psychiatry*, 9:429, 2018.

[11] A. Javaloyes, J. M. Sarabia, R. P. Lamberts, and M. Moya-Ramon. Training prescription guided by heart-rate variability in cycling. *International Journal of Sports Physiology and Performance*, 14(1):23–32, 2019.

[12] V. Kalidas and L. Tamil. Real-time QRS detector using stationary wavelet transform for automated ECG analysis. *Proceedings - 2017 IEEE 17th International Conference on Bioinformatics and Bioengineering, BIBE 2017*, 2018-Janua(512):457–461, 2017.

[13] S. Laborde, A. Brüll, J. Weber, and L. S. Anders. Trait emotional intelligence in sports: A protective role against stress through heart rate variability? *Personality and Individual Differences*, 51(1):23–27, 2011.

[14] R. D. Lane, K. McRae, E. M. Reiman, K. Chen, G. L. Ahern, and J. F. Thayer. Neural correlates of heart rate variability during emotion. *Neuroimage*, 44(1):213–222, 2009.

[15] J. A. Lipponen and M. P. Tarvainen. A robust algorithm for heart rate variability time series artefact correction using novel beat classification. *Journal of Medical Engineering and Technology*, 43(3):173–181, 2019.

[16] F. Liu, C. Liu, X. Jiang, Z. Zhang, Y. Zhang, J. Li, and S. Wei. Performance analysis of ten common QRS detectors on different ECG application cases. *Journal of Healthcare Engineering*, 2018, 2018.

[17] A. Lourenço, H. Plácido da Silva, C. Carreiras, A. Priscila Alves, and A. L. N. Fred. A web-based platform for biosignal visualization and annotation. *Multimedia Tools and Applications*, 70:433–460, 2014.

[18] A. Lourenço, H. Silva, P. Leite, R. Lourenço, and A. Fred. Real Time Electrocardiogram Segmentation For Finger Based ECG Biometrics. 2012.

[19] J. Pan and W. J. Tompkins. Pan Tomkins 1985 - QRS detection.pdf. 32(3):230–236, 1985.

[20] B. Porr and L. Howell. R-peak detector stress test with a new noisy ECG database reveals significant performance differences amongst popular detectors. *bioRxiv*, page 722397, 2019.

[21] D. Saboul, P. Balducci, G. Millet, V. Pialoux, and C. Hautier. A pilot study on quantification of training load: The use of HRV in training practice. *European Journal of Sport Science*, 16(2):172–181, 2016.

[22] D. Sadhukhan and M. Mitra. R-Peak Detection Algorithm for Ecg using Double Difference And RR Interval Processing. *Procedia Technology*, 4:873–877, 2012.

[23] M. Simoons and P. Hugenholtz. Gradual changes of ECG waveform during and after exercise in normal subjects. *Circulation*, 52(4):570–577, 1975.

[24] M. P. Tarvainen, J.-P. Niskanen, J. A. Lipponen, P. O. Ranta-Aho, and P. A. Karjalainen. Kubios hrv–heart rate variability analysis software. *Computer methods and programs in biomedicine*, 113(1):210–220, 2014.

[25] Z. Zhao and Y. Zhang. SQI quality evaluation mechanism of single-lead ECG signal based on simple heuristic fusion and fuzzy comprehensive evaluation. *Frontiers in Physiology*, 9(JUN):1–13, 2018.

[26] J. Zhu, L. Ji, and C. Liu. Heart rate variability monitoring for emotion and disorders of emotion. *Physiological Measurement*, 40(6):064004, 2019.